



## Fused dual boron core based BODIPY dyes: synthesis and optical character



Linlin Wang<sup>a</sup>, Yi Qu<sup>a</sup>, Jingli Xu<sup>a</sup>, Jian Cao<sup>a,\*</sup>, Chunchang Zhao<sup>b,\*</sup>

<sup>a</sup> College of Chemistry and Chemical Engineering, Shanghai University of Engineering Science, Shanghai 201620, PR China

<sup>b</sup> Shanghai Key Laboratory of Functional Materials Chemistry, Key Laboratory for Advanced Materials, and Institute of Fine Chemicals, East China University of Science & Technology, Shanghai 200237, PR China

### ARTICLE INFO

#### Article history:

Received 18 December 2015

Revised 23 February 2016

Accepted 29 February 2016

Available online 3 March 2016

#### Keywords:

BODIPY dyes

Dual boron core

Red-shift emission

Stokes' shift

Schiff's base

### ABSTRACT

Here we report that two boron dipyrromethene derivatives (**BNB-1** and **BNB-2**), bearing double boron atomic centers, have been synthesized and characterized. The additional boron atom was introduced into the skeleton of typical BODIPY dyes through the reaction of  $\text{BF}_3 \cdot \text{Et}_2\text{O}$  and the two ligands, phenol and Schiff's base. The maximum emission wavelength of both dyes moved to 584–603 nm with the larger Stokes' shift ( $\Delta\lambda \approx 40$  nm). Moreover, less solvent polarity dependence of the Stokes' shift ( $40 \pm 6$  nm) was found in different organic solvents. Furthermore, fluorescent lifetime and CV methods were also performed to explore the photophysical and electrochemical behaviors of both dyes.

© 2016 Elsevier Ltd. All rights reserved.

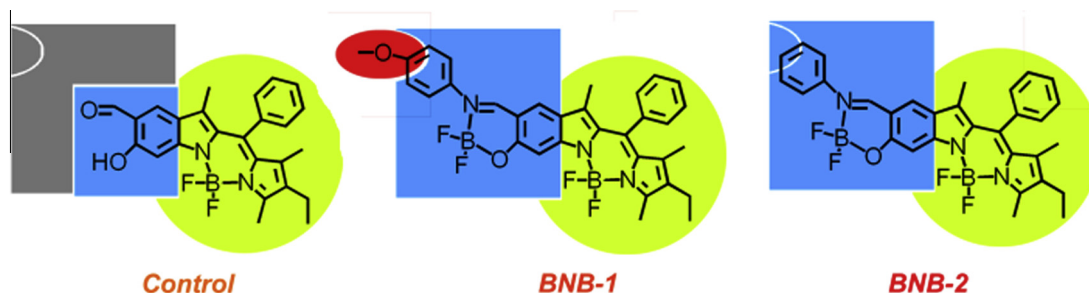
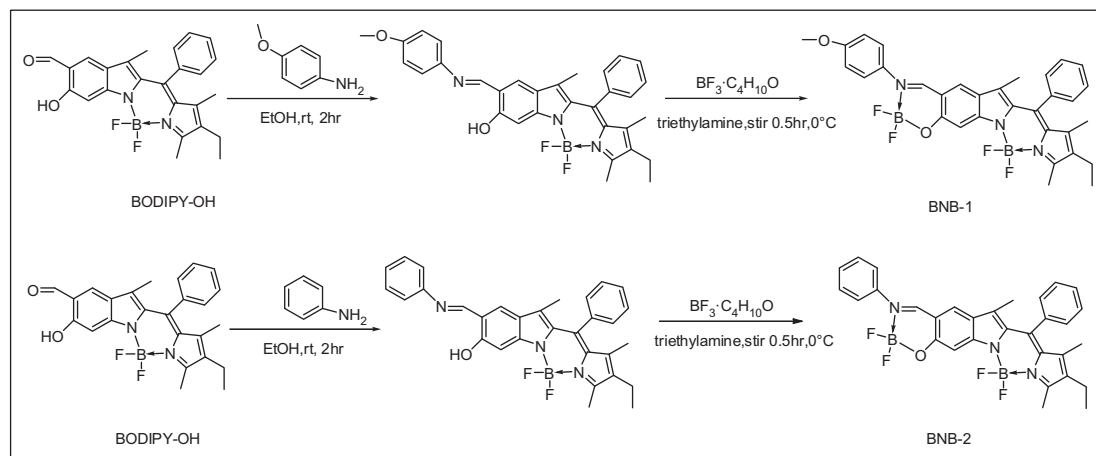
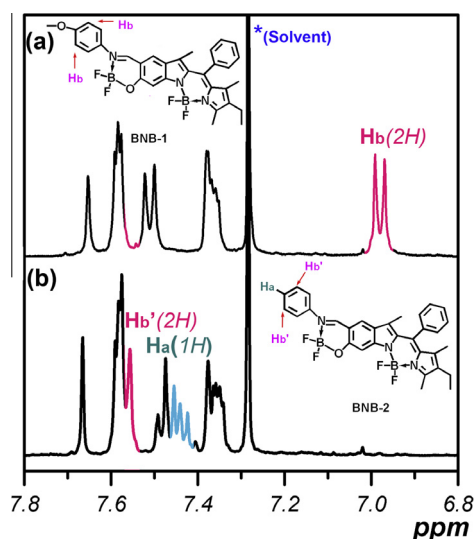
### Introduction

It has been a hot investigation in recent years that the design and synthesis of small-molecular fluorescent dyes are applied for chemosensors, fluorescent label reagents, and nonlinear optical materials. Boron dipyrromethene (BODIPY) and its derivatives are classical organic fluorophores with high luminescent efficiency, relatively sharp fluorescence peaks, and advantageous photostability.<sup>1–5</sup> These BODIPY dyes have worked as energy/electron donors or acceptors in different donor–acceptor sensors. With the demands of the probes or sensitizers in chemosensor and corresponding devices, several modifying strategies about BODIPY dyes were developed: (1) electron-deficient and electron-rich substitutions on the *meso* site of BODIPYs provided the photo-induced electron transfer (PeT) process for designing fluorescent sensors and switches;<sup>6–11</sup> (2) the  $\pi$ -extended BODIPY dyes with longer emission wavelength were obtained by the Knoevenagel reaction or Heck coupling reaction. The formed fluorophores showed deep puncturing depth that is needed for optical bioimaging in vivo;<sup>12–16</sup> (3) Förster resonance energy transfer was another powerful tool to enhance Stokes' shift and construct dual channel detection device. BODIPY can couple with other fluorophores and sensors in order to construct new optical cassettes;<sup>17–19</sup> (4) nucleophilic substitution on the boron core of BODIPY provided plenty

of compounds with different photophysical properties. Until now, the aryl-, alkyl-, alkynyl-, and alkoxy-substituent of BODIPY has been reported in different fields;<sup>20–22</sup> (5) some researches introduced the N atom into the *meso* position of the BODIPY to give the far red/near infrared emission derivatives that could be used as the contrast agents and photodynamic therapy.<sup>23–34</sup>

Because the indole group has larger conjugated system than pyrrole, a series of indole-based BODIPY derivatives have been designed in our previous work.<sup>35</sup> These derivatives with red to near-infrared emission can work as fluorescent probes for different species. However, further exploration in expanding structures and optimizing photophysical properties of these derivatives have not been put forward. Hence, we described a new type of dual boron core BODIPY (**BNB-1** and **BNB-2**) on the basis of indole-based BODIPY, which integrated both typical BODIPYs and mini BODIPY analogs. As shown in Scheme 1, the second boron atom was induced in both dyes to construct the mini BODIPY moiety (blue square), which was fused on the typical BODIPY ring (yellow circle). The newly boron core fixated the Schiff's base and phenol of **BODIPY-OH**, which could keep rigidity and enhance the planarity of the structure. Furthermore, we introduced the methoxy moiety as an electron donor into the *para* position of Schiff's base of **BNB-1**. Then, we employed the <sup>1</sup>H NMR spectra to study the charge distribution on both dyes. UV–vis and emission spectra were employed to explore the behavior of the additional boron unit fused on the BODIPY dyes. The fluorescent quantum yield and lifetime were determined to confirm the role of an electron-rich group ( $-\text{OCH}_3$ )

\* Corresponding authors.

Scheme 1. Structures of the **BNB-1**, **BNB-2**, and control.Scheme 2. Synthesis of **BNB-1** and **BNB-2**.Figure 1. Low-field  $^1\text{H}$  NMR of **BNB-1** and **BNB-2**.

in these BODIPY dyes. Finally, the CV test was also performed to discuss the difference of the electronic properties between **BNB-1** and **BNB-2**.

## Results and discussion

As shown in Scheme 2, **BNB-1** and **BNB-2** were prepared by a simple method. The condensation of the **BODIPY-OH** with the *p*-anisidine and aniline in ethanol under room temperature for 2 h

produced the corresponding Schiff's bases of **BNB-1** and **BNB-2**, respectively. Then, both kinds of the Schiff's bases reacted with  $\text{BF}_3 \cdot \text{OEt}_2$  under ice-bath for half an hour to gain the targets (**BNB-1** and **BNB-2**). The structures of both targets were characterized by  $^1\text{H}$  NMR,  $^{13}\text{C}$  NMR, and HRMS spectra in Supporting information.

Figure 1 described the difference between the  $^1\text{H}$  NMR spectra of **BNB-1** and **BNB-2**. **BNB-1** gave the double peak at high field that assigned to the protons on the phenyl moiety ( $\text{H}_b$ ; 6.95 and 6.97 ppm). Without methoxy group, the corresponding signals of **BNB-2** were found at 7.556 ppm ( $\text{H}_{b'}$ ). Moreover, **BNB-2** had one more proton on the phenyl moiety than **BNB-1**, which could be found at 7.42–7.45 ppm (blue color in Fig. 1b). The HRMS spectrum showed a peak at  $m/z$  584.2303 for **BNB-1** and 554.2175 for **BNB-2** (Figs. S6 and S9), which were consistent with the calculated values (584.2304 for  $[\text{M}-\text{H}]^-$  of **BNB-1** and 554.2198 for  $[\text{M}-\text{H}]^-$  of **BNB-2**).

Compared with the proton  $\text{H}_a$  of **BNB-2** (Fig. 1), the methoxy group of **BNB-1** showed electronic donor property, it caused the difference between **BNB-1** and **BNB-2**. For the investigation of the photophysical properties of **BNB-1** and **BNB-2** in different solvents, UV–vis and fluorescence spectra were performed in Figure 2. As Figure 2a shown, the absorption peak around 350 nm was assigned to the Schiff's base ligand of **BNB-1**. The absorption peak of **BNB-1** was stronger than the one of **BODIPY-OH** that indicated the planarity of **BNB-1** was better than **BODIPY-OH**. The similar phenomenon could also be found in **BNB-2** (Fig. S10).

In Figure 2b, the maximum absorption bands of **BODIPY-OH** shifted from 527 nm to 549 nm with different polarity of solvents. The similar variation was found in **BNB-1** and **BNB-2** but in a longer wavelength region. As shown in Figures 2a and S10e, the maximum absorption bands of **BNB-1** and **BNB-2** ranged from

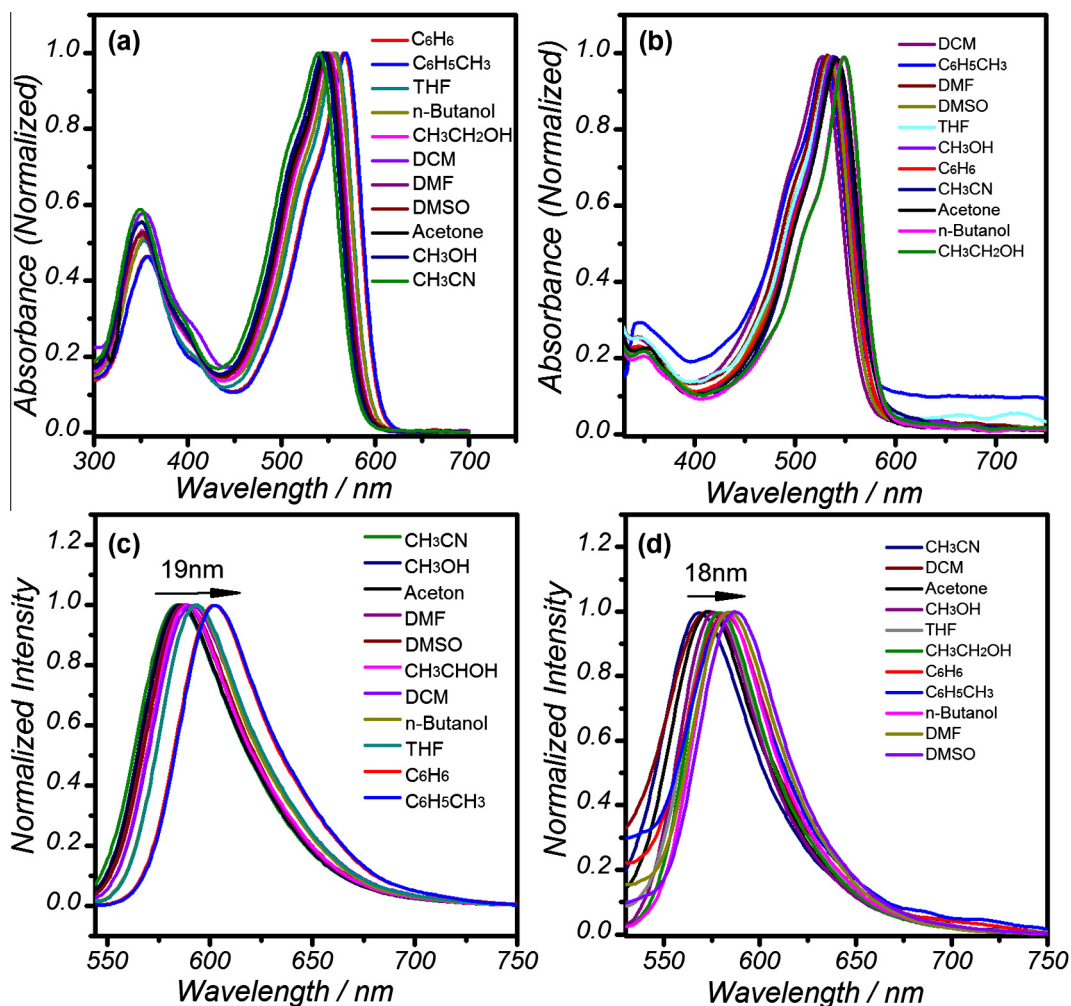


**Figure 2.** In various solvents (a) absorption spectra of **BNB-1**; (b) absorption spectra of **BODIPY-OH**; (c) fluorescence spectra of **BNB-1**; and (d) fluorescence spectra of **BODIPY-OH**.

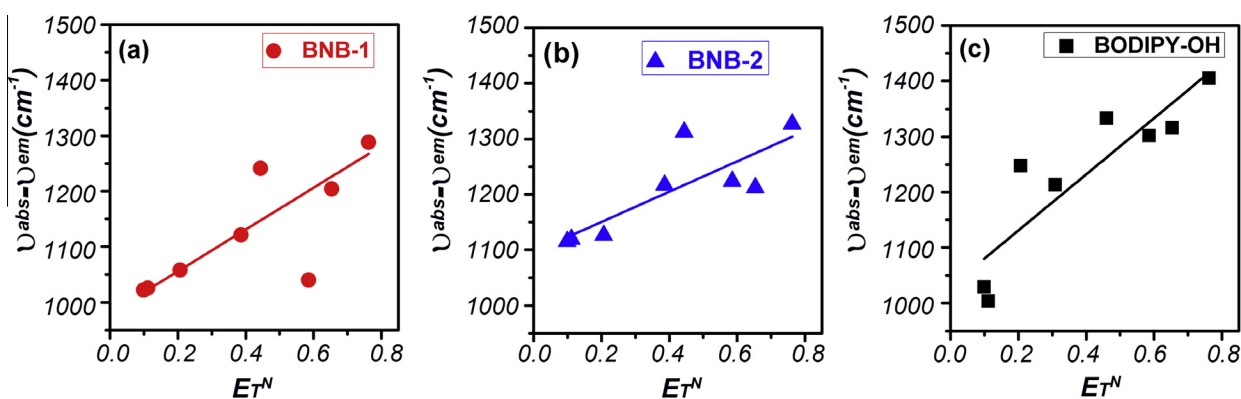


**Figure 3.** Solvachromic effects of **BNB-1** (a), **BNB-2** (b), and **BODIPY-OH** (c).

**Table 1**  
Lifetime and rate constants for radiative and non-radiative deactivation of **BNB-1** and **BNB-2** in  $\text{CH}_2\text{Cl}_2$

	$\tau$ (ns)	$K_r$ ( $10^9 \text{ s}^{-1}$ )	$K_{nr}$ ( $10^9 \text{ s}^{-1}$ )
<b>BNB-1</b>	2.74	0.26	0.11
<b>BNB-2</b>	3.55	0.023	0.26

540 nm to 568 nm and 538 nm to 565 nm, respectively. These evidences implied that the second boron could enlarge the  $\pi$ -extension of BODIPY dyes. But the methoxy group showed little effect in absorption spectra.

Emission spectra were powerful tools for evaluating the new fluorescent dyes. The maximum excitation wavelength is at 530 nm. We detected the emission spectra of **BNB-1**, **BNB-2**, and **BODIPY-OH** in different solvents in Figures 2c, d and S10. **BNB-1**

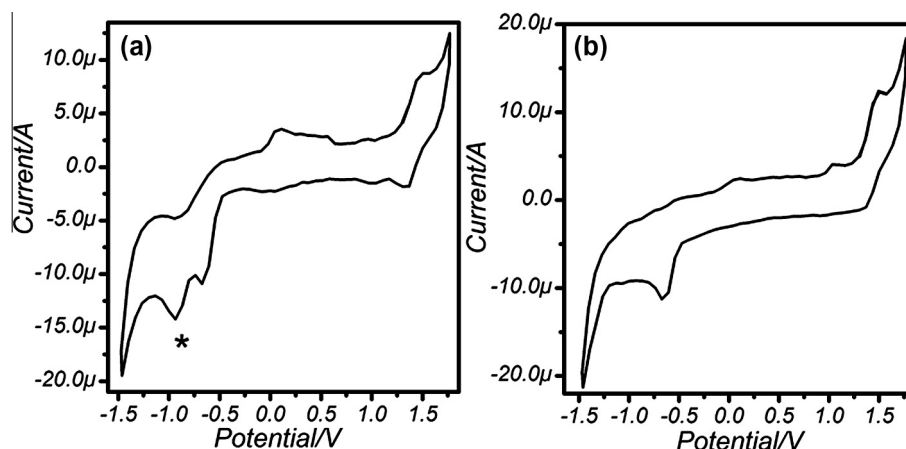


Figure 4. Cyclic voltammogram of **BNB-1** (a) and **BNB-2** (b) in  $\text{CH}_2\text{Cl}_2$  (at  $20 \text{ mV s}^{-1}$ ).

**Table 2**  
Electrochemical data for **BNB-1** and **BNB-2** in  $\text{CH}_2\text{Cl}_2$

Compound	$E_{\text{ox}, 1/2}$ (V) vs ferrocene	$E_{\text{red}, 1/2}$ (V) vs ferrocene
<b>BNB-1</b>	1.42	−0.68/−0.94
<b>BNB-2</b>	1.43	−0.66

exhibited the maximum emission bands, which ranged from 585 nm to 603 nm. **BNB-2** also exhibited the similar variation from 584 nm to 603 nm. The emission bands of **BODIPY-OH** were from 569 nm to 587 nm that showed little hypochromatic shift ( $\Delta\lambda \approx 15 \text{ nm}$ ) than **BNB-1** and **BNB-2**.

Furthermore, fluorescence quantum yield (FQY) of both new dyes were determined with Rhodamine-6G ( $\Phi = 0.94$  in ethanol). The FQY value of **BNB-1** reached 0.71 in dichloromethane, which was much brighter than **BNB-2** ( $\Phi = 0.08$ ). Considered the structures of both dyes, the methoxy group may be responsible for the enhancement of FQY.

The solvent polarity dependence of the fluorophores is more important in fluorescent field than others. The energy of emitting state is more susceptible to the polarity effect that has been known as the solvent relaxation. In order to apply the fluorescent tools in different testing conditions, homeostatic control has been an important parameter for developing the new dyes. Herein, we tested the relation of Stokes' shift (in  $\nu_{\text{abs}} - \nu_{\text{em}}$  form) and solvent polarity parameter (normalized  $E_T$  value). As shown in Figure 3, both **BNB-1** and **BNB-2** showed the smaller variations in Stokes' shift than the control **BODIPY-OH** with the same solvent polarity scales. This consequence illustrated the dual boron core dyes were more beneficial for fluorescent detection in the extensive scales of circumstance.

The fluorescence decay curves of **BNB-1** and **BNB-2** in dichloromethane were given in Figure S11. Both dyes showed the monoexponential decay processes. Based on these curves, the fluorescent lifetime ( $\tau$ ) and related rate constants for radiative and non-radiative deactivation were calculated in Table 1. The fluorescent lifetime of **BNB-1** was 2.74 ns, **BNB-2** showed a little longer value as 3.55 ns than **BNB-1**, and the  $k_f$  value of **BNB-1** was 11 times more than **BNB-2**. These results also proved that the FQY value of **BNB-1** was higher than **BNB-2**.

The cyclic voltammetry test has been performed to explore the impact of methoxy group on these BODIPY dyes (Fig. 4 and Table 2).<sup>36–38</sup> Electrochemical studies of the solutions were performed from  $\sim 0.1 \text{ M}$  analyte compound solutions in dry dichloromethane at  $\nu = 20 \text{ mV s}^{-1}$ . All the electrochemical experiments

were carried out in the three electrode configuration consisting of a Pt button (working electrode), platinum wire (auxiliary electrode), and saturated calomel (reference electrode) electrodes. All potentials were calibrated by the addition of ferrocene as an internal standard, taking  $E_{1/2}(F_c/F_c^+) = 0.42 \text{ V}$ , versus saturated calomel electrode. The supporting electrolyte was  $0.1 \text{ M } [(n\text{-Bu})_4\text{N}][\text{PF}_6]$  ( $\text{TBAPF}_6$ ) that was purified by recrystallization three times from hot ethanol before being dried for three days at  $100\text{--}150^\circ\text{C}$  under active vacuum.<sup>39</sup> The quasi-reversible oxidation processed with half-wave potentials at 1.42 V and 1.43 V were attributed to the oxidation of the **BNB-1** and **BNB-2**, respectively. The irreversible reduction peaks of the **BNB-1** were found at  $-0.68/-0.94 \text{ V}$  and **BNB-2** were found at  $-0.66 \text{ V}$ . Compared to **BNB-2**, **BNB-1** showed an additional reduction peak at  $-0.94 \text{ V}$  (star marker in Fig. 4a), which was considered as another evidence to the individual effect of the methoxy group.

## Conclusions

In this work, two new BODIPY derivatives, **BNB-1** and **BNB-2**, were designed and synthesized. The photophysical and electronic properties of both compounds were investigated. The solvent polarity dependence of the fluorophores was explored by UV-vis and steady-state fluorometric spectra. The fluorescent quantum yield, time-resolved fluorometric spectra, and cyclic voltammetry experiments were performed to discuss the role of the electron donor ( $-\text{OCH}_3$ ) in the new dyes. The FQY value and rate constant for radiative deactivation indicated that the electron donor can optimize the fluorescent property of BODIPY dyes.

## Acknowledgements

This work was partially supported by the NSFC/China (21404068), the talent programs from Shanghai Education Commission (ZZGCD15029), and SUES (A1-5300-14-020303).

## Supplementary data

Supplementary data associated with this article can be found, in the online version, at <http://dx.doi.org/10.1016/j.tetlet.2016.02.109>.

## References and notes

- Ulrich, G.; Ziesel, R.; Harriman, A. *Angew. Chem., Int. Ed.* **2008**, *47*, 1184.
- Shao, J. Y.; Sun, H. Y.; Guo, H. M.; Ji, S. M.; Zhao, J. Z.; Wu, W. T.; Yuan, X. L.; Zhang, C. L.; James, T. D. *Chem. Sci.* **2012**, *3*, 1049.

3. Zhang, C. S.; Zhao, J. Z.; Wu, S.; Wang, Z. L.; Wu, W. H.; Ma, J.; Guo, S.; Huang, L. *J. Am. Chem. Soc.* **2013**, *135*, 10566.
4. Boens, N.; Leen, V.; Dehaen, W. *Chem. Soc. Rev.* **2012**, *41*, 1130.
5. Loudet, A.; Burgess, K. *Chem. Rev.* **2007**, *107*, 4891.
6. Zhao, W.; Carreira, E. M. *Angew. Chem., Int. Ed.* **2005**, *44*, 1677.
7. Sunahara, H.; Urano, Y.; Kojima, H.; Nagano, T. *J. Am. Chem. Soc.* **2007**, *129*, 5597.
8. Ueno, T.; Urano, Y.; Kojima, H.; Nagano, T. *J. Am. Chem. Soc.* **2006**, *128*, 10640.
9. Shie, J. J.; Liu, Y. C.; Lee, Y. M.; Lim, C.; Fang, J. M.; Wong, C. H. *J. Am. Chem. Soc.* **2014**, *136*, 9953.
10. Dost, Z.; Atilgan, S.; Akkaya, E. U. *Tetrahedron* **2006**, *62*, 8484.
11. Qi, X.; Jun, E. J.; Xu, L.; Kim, S. J.; Hong, J. S. J.; Yoon, Y. J.; Yoon, J. Y. *J. Org. Chem.* **2006**, *71*, 2881.
12. Yu, Y. H.; Descalzo, A. B.; Shen, Z.; Rohr, H.; Liu, Q.; Wang, Y. W.; Spieles, M.; Li, Y. Z.; Rurack, K.; You, X. Z. *Chem. Asian J.* **2006**, *1*, 176.
13. Frenette, M.; Hatamimoslehabadi, M.; Bellinger-Buckley, S.; Laoui, S.; La, J.; Bag, S.; Mallidi, S.; Hasan, T.; Bouma, B.; Chandra Yelleswarapu, C.; Rochford, J. *J. Am. Chem. Soc.* **2014**, *136*, 15853.
14. Wakamiya, A.; Sugita, N.; Yamaguchi, S. *Chem. Lett.* **2008**, *37*, 1094.
15. Rohand, T.; Qin, W.; Boens, N.; Dehaen, W. *Eur. J. Org. Chem.* **2006**, *20*, 4658.
16. Qin, W.; Rohand, T.; Dehaen, W.; Clifford, J. N.; Driesen, K.; Beljonne, D.; Van Averbek, B.; Van der Auwerda, M.; Boens, N. *J. Phys. Chem. A* **2007**, *111*, 8588.
17. Yuan, M. J.; Zhou, W. D.; Liu, X. F.; Zhu, M.; Li, J. B.; Yin, X. D.; Zheng, H. Y.; Zuo, Z. C.; Ouyang, C. B.; Liu, H. B.; Li, Y. L.; Zhu, D. B. *J. Org. Chem.* **2008**, *73*, 5008.
18. Luo, L.; Wu, D.; Li, W.; Zhang, S.; Ma, Y. H.; Su Yan, S.; You, J. S. *Org. Lett.* **2014**, *16*, 6080.
19. Cheng, T. Y.; Wang, T.; Zhu, W. P.; Chen, X. L.; Yang, Y. J.; Xu, Y. F.; Qian, X. H. *Org. Lett.* **2011**, *13*, 3656.
20. Zhao, N.; Xuan, S.; Fronczek, F. R.; Smith, K. M.; Vicente, M. G. H. *J. Org. Chem.* **2015**, *80*, 8377.
21. Sánchez-Carnerero, E. M.; Moreno, F.; Maroto, B. L.; Agarrabeitia, A. R.; Ortiz, M. J.; Vo, B. G.; Muller, G.; De la Moya, S. *J. Am. Chem. Soc.* **2014**, *136*, 3346.
22. Bandi, V.; Das, S. K.; Awuah, S. G.; You, Y. J.; D'Souza, F. J. *Am. Chem. Soc.* **2014**, *136*, 7571.
23. Zhu, H.; Fan, J. L.; Wang, J. Y.; Mu, H. Y.; Peng, X. J. *J. Am. Chem. Soc.* **2014**, *136*, 12820.
24. Adarsh, N.; Krishnan, M. S.; Ramaiah, D. *Anal. Chem.* **2014**, *86*, 9335.
25. Xinfu Zhang, X. F.; Haibo Yu, H. B.; Xiao, Y. J. *Org. Chem.* **2012**, *77*, 669.
26. Zhang, X. X.; Wang, Z.; Yue, X. Y.; Ma, Y.; Kieseewetter, D. O.; Chen, X. Y. *Mol. Pharm.* **2013**, *10*, 1910.
27. Sun, H. B.; Dong, X. C.; Liu, S. J.; Zhao, Q.; Mou, X.; Hui Ying Yang, H. Y.; Huang, W. J. *Phys. Chem. C* **2011**, *115*, 19947.
28. Coskun, A.; Yilmaz, M. D.; Akkaya, E. U. *Org. Lett.* **2007**, *9*, 607.
29. Killoran, J.; Allen, L.; Gallagher, J. F.; Gallagher, W. M.; O'Shea, D. F. *Chem. Commun.* **2002**, 1862.
30. McDonnell, S. O.; Hall, M. J.; Allen, L. T.; O'Shea, D. F. *J. Am. Chem. Soc.* **2005**, *127*, 16360.
31. Gorman, A.; Killoran, J.; O'Shea, C.; Kenna, T.; Gallagher, W. M.; O'Shea, D. F. *J. Am. Chem. Soc.* **2004**, *126*, 10619.
32. Wang, H.; Zeng, J. *Can. J. Chem.* **2009**, *87*, 1209.
33. Aznar, F.; Valdes, C.; Cabal, M. P. *Tetrahedron Lett.* **2000**, *41*, 5683.
34. Chen, J.; Burghart, A.; Wan, C. W.; Thai, L.; Ortiz, C.; Reibenspies, J.; Burgess, K. *Tetrahedron Lett.* **2000**, *41*, 2303.
35. Cao, J.; Zhao, C. C.; Wang, X. Z.; Zhang, Y. F.; Zhu, W. H. *Chem. Commun.* **2012**, 9897.
36. Ziessel, R.; Goze, C.; Ulrich, G.; Cesario, M.; Retailleau, P.; Harriman, A.; Rostron, J. P. *Chem. Eur. J.* **2005**, *11*, 7366.
37. Gabe, Y.; Ueno, T.; Urano, Y.; Kojima, H.; Nagano, T. *Anal. Bioanal. Chem.* **2006**, *386*, 621.
38. Burghart, A.; Kim, H.; Weich, M.; Thoresen, L. H.; Reibenspies, J.; Burgess, K.; Bergström, F.; Johansson, B. A. *J. Org. Chem.* **1999**, *64*, 7813.
39. Khan, T. K.; Ravikanth, M. *Tetrahedron* **2011**, *67*, 5816.